J Mater Sci (2010) 45:5271–5281
DOI 10.1007/s10853-010-4570-9

Study of structural change in Wyodak coal in high-pressure CO_2 by small angle neutron scattering

Mojtaba Mirzaeian · Peter J. Hall · Hasan Fathinejad Jirandehi

Received: 26 January 2010 / Accepted: 27 April 2010 / Published online: 4 June 2010

Abstract Small angle neutron scattering (SANS) has been applied to examine the effect of high-pressure CO_2 on the structure of Wyodak coal. Significant decrease in the scattering intensities on the exposure of the coal to high-pressure CO_2 showed that high-pressure CO_2 rapidly gets adsorbed on the coal and reaches to all the pores in the structure. This is confirmed by strong and steep exothermic peaks observed on DSC scans during coal/CO_2 interactions. In situ small angle neutron scattering on coal at high-pressure CO_2 atmosphere showed an increase in scattering intensities with time suggesting that after adsorption, high-pressure CO_2 immediately begins to diffuse into the coal matrix, changes the macromolecular structure of the coal, swells the matrix, and probably creates microporosity in coal structure by extraction of volatile components from coal. Significant decrease in the glass transition temperature of coal caused by high-pressure CO_2 also confirms that CO_2 at elevated pressures dissolve in the coal matrix, results in significant plasticization and physical rearrangement of the coal's macromolecular structure.

Introduction

The anticipated doubling of world energy consumption within the next 50 years [1] and associated emissions from the use of fossil fuels as a primary energy provider suggest that the concentration of CO_2 in the atmosphere will continue to increase. Excluding water vapor, CO_2 from combustion of fossil fuels is the most abundant greenhouse gas that has been produced by anthropogenic activities contributing to the greenhouse effect by 63.6% up to now [2]. Therefore, in order to stabilize the atmospheric concentration of greenhouse gases, significant steps are required to reduce the release of carbon dioxide (CO_2) into the atmosphere.

CO_2 sequestration can be defined as the capture and secure storage of CO_2 that would otherwise be emitted to or remain in the atmosphere. The captured CO_2 could be concentrated into a liquid or gas stream that could be transported and injected into deep underground geological formations. Geological formations, such as oil fields, deep coal beds, and aquifers, are likely to provide the first large-scale opportunity for concentrated sequestration of CO_2.

Storage within coal seams is one of the most attractive opportunities for long-term sequestration of large volume of anthropogenic CO_2 [3–5] due to the following reasons:

- CO_2 sorption into coal is high, and coal has the ability to adsorb large volumes of CO_2 in a highly concentrated state [6].
- CO_2 sorption is effective at displacing CH_4 from coal beds, and the valuable CH_4 can be produced. The displacement of CH_4 by CO_2 is achieved due to the preferential sorption of CO_2 on coal under the operational conditions [7, 8].
- Unmineable deep coal beds, which are the best sites for sequestration, are frequently located near large point sources of CO_2 emissions, especially power generation plants.

CO_2 is a fluid that like organic solvents can dissolve in the organic coal matrix, changing coals' physical structure,

M. Mirzaeian (✉) · P. J. Hall
Department of Chemical and Process Engineering, University of Strathclyde, Glasgow G1 1XJ, Scotland, UK
e-mail: mojtaba.mirzaeian@strath.ac.uk

H. F. Jirandehi
Department of Chemistry, Azad University Farahan Branch, Arak, Iran

properties, and behavior [9–13]. In order to obtain an improved understanding of the sequestration process and long-term effects of sequestration, it is worthwhile to find information on the interactions of CO_2 with coals and the effects of CO_2 on coals' properties.

CO_2 injection into, and CH_4 recovery from coal seams will use high-pressure techniques, and little is known about the high-pressure interactions of coal and CO_2. In order to determine which coal seams would be good disposal sites and under what environmental conditions the sequestered CO_2 would remain stable in coal, a better understanding of the high-pressure interactions of coal and CO_2 is essential. Analysis of coal/CO_2 interactions data includes both structural and chemical information which cannot easily be separated from one another. Studies of the void structure of coals can provide important information which, together with kinetic studies of coal/CO_2 interactions, gives a picture that the adsorbed molecules have specific interactions with the internal surface or have significant solubility in the organic matrix.

Coal is a chemically heterogeneous solid containing mainly carbonaceous material with a very low amount of mineral mater. It is a three-dimensionally crosslinked macromolecular structure with a wide range of highly reactive chemical functional groups [14]. It is well known that solvents such as pyridine, which break hydrogen bonds, swell but do not completely dissolve coal [15]. There is some evidence to show that coal can swell in high-pressure CO_2, presumably due to the quadrupolar nature of the molecule disrupting weak electrostatic bonds within the coal structure. Dilatometric studies on coals in contact with CO_2 showed significant increase in sample size [10–12]. In the most significant study of coal behavior in high-pressure CO_2 atmospheres, Reucroft and Sethuraman [12] have shown that coals swell after exposure to CO_2, and the amount of swelling increases with increasing pressure. In our previous study [16], we studied the structural change in different coals under high-pressure CO_2, and showed that CO_2 at higher pressures diffuses through the coal matrix, causes significant plasticization effects, and changes the macromolecular structure of the coal.

In this study, we have applied small angle neutron scattering and differential scanning calorimetry (DSC) to examine structural changes in Wyodak coal at high-pressure CO_2 atmosphere.

The CO_2 storage capacity of unmineable coal seams in the United States is estimated as 90 Gt CO_2 and among them, unmineable coal seams within the Power River Basin of Wyoming and Montana are capable of storing 14 Gt CO_2 [17]. Wyodak coal is one of the major coal seams with the largest coal resource in the Powder River Basin and is the largest coal-producing bed in the United States. It is sub-bituminous with an average BTU of 8,220 (8666 kJ), ash of 6.0%, and sulfur of 0.50% [18]. Because of its large CO_2 sequestration potential, injecting CO_2 into the unmineable Wyodak coal seam is of interest and can provide a significant potential storage medium for CO_2 emissions.

The results obtained from this study help to understand the mechanism of coal/CO_2 interactions and to gain information about how and where CO_2 is stored at elevated pressures within the coal's macromolecular structure.

SANS theory

Small angle scattering from porous solids arises from the changes in scattering density due to the interface between the solid and the pores [19]. In a SANS experiment, the intensity of scattered neutrons $I(q)$ is measured as a function of scattering angle from the incident beam, or alternatively, as a function of the scattering wave vector q.

The scattering wave vector, q, is the difference between the vectors of incident beam and scattered neutrons and is defined by:

$$q = \frac{4\pi}{\lambda}\sin(\theta) \tag{1}$$

where λ is the neutron wavelength, and θ is half of scattering angle. The general equation for determining the intensity of scattering is

$$I(q) = I_0(\lambda)\,\Delta(\Omega)\,\eta(\lambda)\,\Gamma(\lambda)\,V_s\frac{d\Sigma}{d\Omega}(q) \tag{2}$$

where I_0 is the incident flux; $\Delta\Omega$ is the solid angle element; η is the detector efficiency; Γ is the neutron transmission of the sample, and V_s is the volume of the sample exposed to the neutron beam [20].

The first three terms in Eq. 2 are instrument specific, whereas the last term is sample dependent and is known as the differential cross section. Because the differential cross section contains all the information on the size, shape, and interactions between the scattering centers in the sample, the objective of a SANS experiment is to determine differential cross section. A generalized expression for the SANS from a sample can be written as follows [21]:

$$\frac{d\Sigma}{d\Omega}(q) = (\rho_m - \rho_p)^2 \int N_0 G(q,R)\,[V(R)]^2 f(R)\,dR \tag{3}$$

where N_0 is the number density of scattering centers, $G(q, R)$ is the scattering kernel, $V(R)$ is the volume of the scattering centers, and $f(R)$ is the normalized size distribution of scattering centers.

The term $(\rho_m - \rho_p)^2$ is the square of the difference in neutron scattering length density of the two phases (particles or pores and matrix). This term is known as contrast and is the key parameter to determining the intensity of scattering.

There are two contributions to the measured signal due to coherent and incoherent scattering.

$$\frac{\partial \Sigma}{\partial \Omega}(q) = \frac{\partial \Sigma_{\text{coh}}}{\partial \Omega}(q) + \frac{\partial \Sigma_{\text{Inc}}}{\partial \Omega}(q) \tag{4}$$

Incoherent scattering is independent of angle and thus is not q-dependent and contributes only to the noise level.

In a SANS experiment, on completion, data are reduced into ($d\Sigma/d\Omega$) versus q. Then, structural information about the matrix and included void volumes can be extracted by applying an appropriate method of data analysis. The main steps in data reduction are normalization and removal of incoherent background before interpreting the data and fitting them to an appropriate model.

The Guinier approximation and Porod's law

The Guinier approximation relies on the fact that limiting behavior in the low-q range of the scattering is not independent of the size and shape of the scatterers. Guinier has shown that for a system of monodisperse heterogeneities, at small values of q, the scattering intensity may be related to the radius of gyration of the scatterer by an exponential function of the form [22, 23]:

$$\lim_{q \to 0} I(q) = I(0) \exp\left(-\frac{q^2 R_g^2}{3}\right) \tag{5}$$

where $I(0)$ is the incident neutron flux, and R_g is radius of gyration, which is defined as the mean distance from the center of gravity. For a monodisperse system of spheres having a radius R_s, a plot of ln $I(q)$ versus q^2 will yield a straight line at low q, from which radius of gyration can be obtained from the gradient. For spheres, R_g is simply related to the dimension of the scattering particles (or void), or geometrical radius by:

$$R_g = \sqrt{(3/5)} R_s \tag{6}$$

In the case of monodisperse systems having non-spherical shapes, the relationship of R_g to geometrical characteristics of the scatters is more complicated. The Guinier approximation is generally valid for $qR_g < 1$ within the q range in which R_g is determined.

For a complex system such as coal, the heterogeneities are polydisperse in form and size [24], the Guinier plot will not be linear, and thus R_g does not have a single value, and indicates a distribution. In order to estimate the intercept and approximate the shape of the low q region of the scattering curve, Guinier plots were fitted to a polynomial in q [22, 24].

$$\ln I(q) = A - B_1 q + B_2 q^2 - B_3 q^3 + B_4 q^4 \tag{7}$$

and then the average value of R_g is given by

$$R_g = \sqrt{3B_2} \tag{8}$$

If the boundary between the scattering objects and the matrix is sharp, and there is a random distribution of heterogeneities of scattering length density, then the behavior of the scattering varies proportional to q^{-4} at higher q ranges, and scattering is proportional to the total interface surface area between the two homogeneous media. Then, the scattering intensity will obey Porod's law [23, 25]:

$$\lim_{q \to \infty} I(q) = (\rho_m - \rho_p)^2 \frac{2\pi}{q^4} S \tag{9}$$

where S is the total interfacial surface area of the illuminated volume of sample, ρ_m and ρ_p are the scattering length densities of matrix and particles (voids), respectively. Equation 9 predicts that the absolute intensity of scattering in high q region is dependent on only two parameters of the system: the difference in scattering length density between the two phases, and the total surface area of the interface between the two phases, S. Porod behavior is valid only in the limit $qr \gg 1$ where r is the radius of the structure resulting in the scattering. The Porod's law can be used to measure the surface area of domains in the nano-scale. The calculation of the surface area is valid for structures of all geometries [24].

For a two-phase system, the integrated scattering intensity is related to the volume fraction by

$$\int_0^\infty \frac{d\Sigma}{d\Omega} q^2 dq = 2\pi^2 (\rho_m - \rho_p)^2 \varphi (1 - \varphi) \tag{10}$$

where φ is the volume fraction of particles (voids) in matrix. The integral on the left-hand side of Eq. 10 can be estimated from scattering data provided over a sufficiently wide q. Extrapolations can be performed by the Guinier approximation, Eq. 5, or Eq. 7 for the $q \to 0$ limit, and by Porod's law, Eq. 9 for the $q \to \infty$ limit.

Experimental

Wyodak coal obtained from the Argonne Premium Coal Sample Program was used in this study. Wyodak is a sub-bituminous coal and the complete analysis of the coal sample, such as proximate analysis, elemental analysis, and pore analysis are given in Table 1, and in the "BET analysis" section.

BET analysis

The porosity of the Wyodak coal sample was studied by the analysis of nitrogen adsorption–desorption isotherms measured by an ASAP 2420 adsorption analyzer (Micromeritics) at 77 K. The sample was evacuated at 373 K for 2 h prior to the adsorption measurements. BET method was used

Table 1 Approximate and elemental analysis of the coal sample

Coal	Approximate analysis (wt%)				Elemental analysis (daf %)				
	MC	FC	VM	Ash	C	H	O[a]	N	S
Wyodak	19.9	38.4	35.7	5.9	79.81	5.69	12.57	1.19	0.74

MC moisture content, *FC* fixed carbon, *VM* volatile matter

[a] By difference

for surface area measurements, BJH adsorption–desorption was used for mesopore analysis and average pore diameter. Total pore volume was calculated from the adsorbed volume of nitrogen at $P/P_0 = 0.99$ (saturation pressure). Pore size distribution (PSD) was obtained by the BJH method from adsorption branch of the isotherms [26].

Adsorption–desorption isotherms of nitrogen on the Wyodak coal sample are shown in Fig. 1. The isotherms show a hysteresis loop with type-IV isotherm which is representative of the filling and emptying of mesopores in the P/P_0 region of 0.2–0.98 by capillary condensation of the adsorbate in the pores of the solid. This suggests the mesoporosity in the solid [27].

The lower part of the hysteresis loop represents the filling of the mesopores, while the upper part represents the emptying of the mesopores.

Figure 2 shows PSD curve for the coal sample calculated using the BJH method. The obtained PSD curve indicates that the coal structure is dominated by mesopores. Specific surface area S_{BET}, total pore volume, and average pore diameter for Wyodak coal sample are 3.7 m^2/g, 0.015 cm^3/g, and 17.13 nm, respectively.

SANS measurements

Small angle neutron scattering experiments were performed at the ISIS spallation neutron source at the Rutherford Appleton Laboratories, Chilton, Didcot in the United Kingdom. This is a time-of-flight source, and the small angle instrument (LOQ) uses neutrons over the wavelength range 2.2–10 Å. With this wavelength range, LOQ offers a very wide range of scattering wave vector q. The sample holder consisted of two optically transparent windows made from sapphire with a path length of 0.2 cm. This assembly was placed in a high-pressure cell. Typical SANS experiments were as follows:

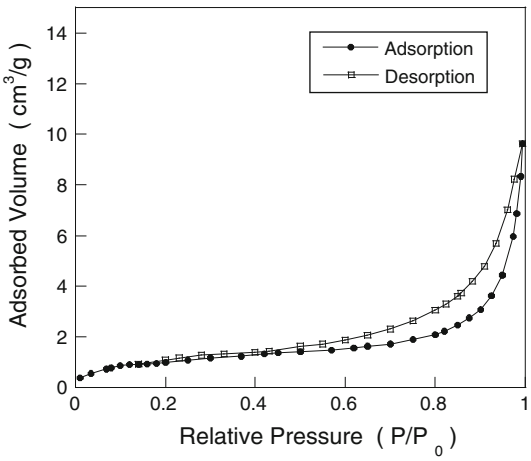

Fig. 1 Adsorption/desorption isotherms of N_2 at 77 K on Wyodak coal sample

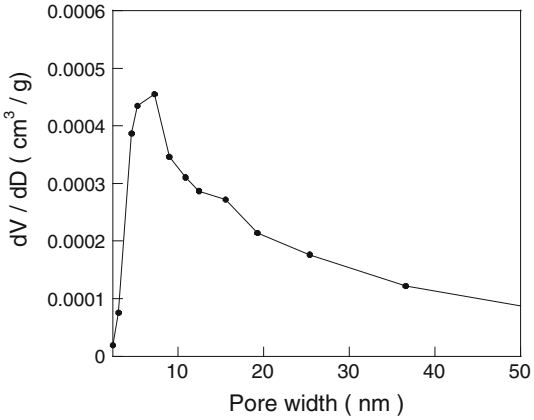

Fig. 2 Pore size distribution of Wyodak coal sample

In the first experiment, the coal sample was contained in the high-pressure optical cell (no CO_2), and SANS was performed with transmission time of 15 min, and scattering time of 10 min.

In the second experiment, the coal sample was placed in the high-pressure optical cell, and CO_2 was transmitted from a high-pressure CO_2 cylinder within the cell. The pressure was controlled by a pressure transducer at a desired pressure, and the sample was under this pressure for 24 h prior to the SANS experiment. Then, SANS was performed with transmission time of 15 min, and scattering time of 10 min. This experiment was repeated for different CO_2 pressures.

In the third set of experiments, SANS was performed in situ on the coal sample at high-pressure CO_2 atmosphere. The high-pressure CO_2 was introduced rapidly on the fresh coal sample contained in the high-pressure optical cell at a desired pressure controlled by pressure transducer, and $I(q)$ was then measured every 10 min with transmission time of 15 min, and scattering times of 10 min.

In each experiment, data were collected and then reduced. Data reduction consists of the correction of the scattering data for scattering from empty cell or gas-filled cell, transmitted beam, and other instrumental backgrounds.

Differential scanning calorimetry measurements

The DSC measurements were performed with a Mettler DSC 30 instrument using standard aluminum pans with

two pinholes to minimize mass transfer limitations in evaporation of water, or contact of gas with sample during DSC scans. Nitrogen flowing at 10 mL/min was used as a carrier gas to keep the cell free of oxygen during measurements. Typically, 10 mg of sample was used in an experiment. The DSC measurements were performed at a heating rate of 10 °C/min. Cooling of the furnace between consecutive heating scans was carried out using a liquid nitrogen cooling accessory directly beneath the furnace.

CO_2 adsorption on coal

In order to study the adsorption of CO_2 on the coal, DSC scans were conducted on the Wyodak coal sample as follows:

A sample of fresh coal was purged with N_2 flowing at 10 mL/min for 10 min in DSC chamber, then heated to 110 °C at 10 °C/min, and held for 30 min, cooled at nominal rate of 100 °C/min to −60 °C under N_2 flowing at 10 mL/min. At this point, gas was switched to CO_2, and the sample was then immediately heated from −60 to 200 °C under CO_2 flowing at 10 mL/min at 10 °C/min three times in succession with a cooling rate of 10 °C/min between heating runs.

Effect of high-pressure CO_2 on the coal structure

In order to study the effect of high-pressure CO_2 on the macromolecular structure of Wyodak coal, DSC scans were conducted as follows:

(1) A sample of Wyodak coal was purged with N_2 flowing at 10 mL/min for 10 min in DSC chamber, then heated from 30 to 110 °C at a heating rate of 10 °C/min, held at 110 °C for 30 min, and cooled to 30 °C in N_2 atmosphere at a flow rate of 10 mL/min. The dried sample was heated from 30 to 200 °C at 10 °C/min in N_2 atmosphere flowing at 10 mL/min three times in succession. This experiment was carried out to determine the phase transitions of Wyodak coal in N_2 atmosphere.
(2) A sample of Wyodak coal was purged with 20 bar Ar three times in succession, to flush adsorbed gases present in the pores in coal and also oxygen form the high-pressure cell completely as Ar has a better access to the coal's pore structure compared to N_2; then the sample was heated to 110 °C, held for 30 min at 110 °C, and cooled to 30 °C at 10 °C/min under Ar atmosphere in the high-pressure cell. The dried sample was exposed to CO_2 at the desired pressure at room temperature for 24 h. After that, the CO_2 pressure was rapidly released, the sample was purged with 20 bar Ar, and transferred to the DSC chamber. The sample was purged with N_2 with a flow rate of 10 mL/min for 10 min in the DSC chamber, and DSC was carried out from 30 to 200 °C at 10 °C/min in N_2 atmosphere three times in succession. The purpose of this sequence was to determine the effect of high-pressure CO_2 atmospheres on the phase transition of the coal sample.

Results and discussion

SANS results

This section considers the analysis of SANS data to obtain structural information about the matrix and the included void volume of coal samples at high-pressure CO_2. After the experiment was completed, the data were reduced by subtracting the effects of empty or gas-filled cell, transmitted beam, and other instrumental backgrounds. Correction for incoherent scattering was made by assuming that at the largest scattering wave vector, the scattering was q independent and dominated by incoherent effects.

Incoherent background correction

Coal is a chemically heterogeneous solid containing mainly carbonaceous matter with various amounts of mineral matter. Mineral mater present in coal contributes less to the SANS because the scattering cross section of the mineral elements studied here are similar to the cross section of the carbonaceous matrix [24]. Coal samples contain a large amount of hydrogen in the organic matrix. As it can be determined from data given in Table 1, the mole fraction of hydrogen in coal samples accounts for approximately 45% of all the atoms obtained from elemental analysis based on moisture and ash free.

Hydrogen possesses a large incoherent scattering cross section, and hydrogenated samples exhibit low transmissions, great absorbances, and large incoherent backgrounds [20]. Incoherent scattering intensities depend not on the sample's structure but only on the contents of elements in the neutron beam pathway [28]. The incoherent scattering from the hydrogen and density variations due to the organic matrix inhomogeneities should scatter uniformly into the entire q range. Thus, the principal effect of hydrogen should be to contribute a uniform background term to the measured q-dependent intensity in the whole q range. At high q region, the scattering intensities are q independent and dominated by incoherent effects. Therefore, the high q limiting intensities, corresponding approximately to the incoherent scattering, were subtracted from the background subtracted intensities to give $I_{coh}(q)$ prior to

analysis [21]. This incoherent background correction was performed for all scattering curves prior to analysis.

Scattering from the coal before and after exposure to CO_2 at different pressures

Figure 3 shows the results of scattering from a fresh coal sample. Different regions of the scattering curve can provide information about the different features of the coal structure. A linear region for a limited range of q values indicates that this scattering regime exhibits power law behavior with increasing q. This is due to scattering from meso- and macroporosity and can be interpreted as arising from pores having a fractal surface (surfaces having no characteristic length but having dimensions only in a limited size region) [29, 30] or arising from a irregular distribution of mass (mass fractal).

In evaluating fractal dimensions, the scattering curve is fitted to a fractal model (linear function), and the dimensionality of surface is estimated by subtracting the slope from 6, $D_s = (6 - \text{slope})$, and the dimensionality of mass is equal to the slope, $D_m = \text{slope}$ [30–33].

The scattering pattern of the Wyodak coal shown in Fig. 3 has a linear behavior in the region $q < 0.017$ Å^{-1} with a slope of -2.6. This is related to a mass fractal dimensionality of 2.6 and shows that the scattering in this region might have arisen from fractal distribution of mass or density fluctuations (scattering from a mass fractal). The upward deviation from the linear scattering for $q > 0.017$ Å^{-1} suggests microporosity in the Wyodak coal structure [32]. The slopes and fractal dimensions are given in Table 2.

Figure 4 shows the small angle neutron scattering patterns of the Wyodak coal at various CO_2 pressures. The drastic reduction in the scattering intensities for coal at high-pressure CO_2 compared with the intensities for fresh coal might be attributed to the reduction in the scattering contrast between pores and coal matrix due to the adsorption of CO_2

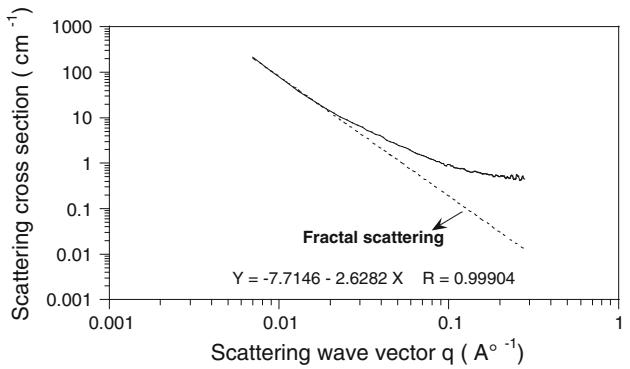

Fig. 3 Power law plot of the small angle neutron scattering for Wyodak coal sample

Table 2 SANS characteristics of the Wyodak coal at various CO_2 pressures

CO_2 pressure (bar)	D_m	R_g (Å)	R_s (Å)	Q (arb. units)
0	2.62	197.70	255.23	0.0002064
15	2.58	205.79	256.67	0.0004880
25	2.56	238.64	308.08	0.0007523

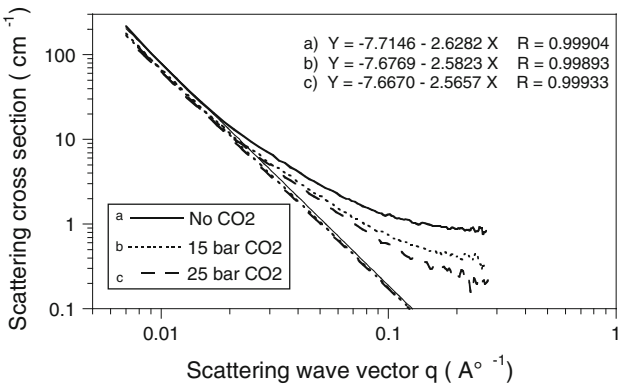

Fig. 4 Small angle neutron scattering patterns for Wyodak coal at various CO_2 pressures

within the pores. It can be observed that the scattering intensities decrease with CO_2 pressure in the entire q range. This suggests that as CO_2 is adsorbed into pores the scattering contrast between pore and coal, $[(\rho_m - \rho_p)^2]$, will be reduced and the amount of reduction in the scattering contrast increases with CO_2 pressure due to the increase in the scattering length density of CO_2 with pressure.

The SANS results also show that the amount by which scattering is reduced varies as a function of scattering wave vector q. This might be related to the variations of the density of adsorbed CO_2 with pore size. It has been suggested that the density of CO_2 is a function of pore size, and as CO_2 is adsorbed in pores, it interacts with two pore walls and will be subjected to large interaction energy or effectively a large pressure [34].

Figure 4 shows that for fresh Wyodak coal scattering in the region $q < 0.017$ Å^{-1} is linear, suggesting scattering from a fractal structure. For Wyodak coal loaded with 15 bar CO_2, scattering in the region $q < 0.02$ Å^{-1} is fractal, and for Wyodak coal loaded with 25 bar CO_2, fractal scattering happens in the region $q < 0.023$ Å^{-1}. The extension of fractal scattering region with CO_2 pressure might be associated with the increase in size of pores due to the swelling of coal with high-pressure CO_2. In all the curves, an upward deviation in the scattering patterns shows the presence of microporosities in the coal structure [35]. Linear region for each curve is fitted to a fractal model, and the results of fitting are given in Table 2. In all the cases, linear scattering is related to a mass fractal arising from fractal distribution of mass or density fluctuations.

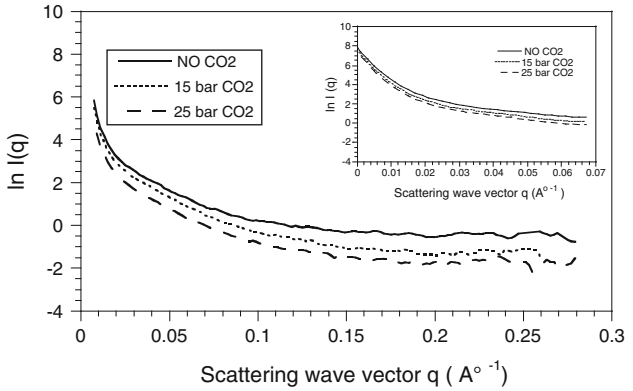

Fig. 5 Guinier plot of the small angle neutron scattering for Wyodak coal at various CO_2 pressures

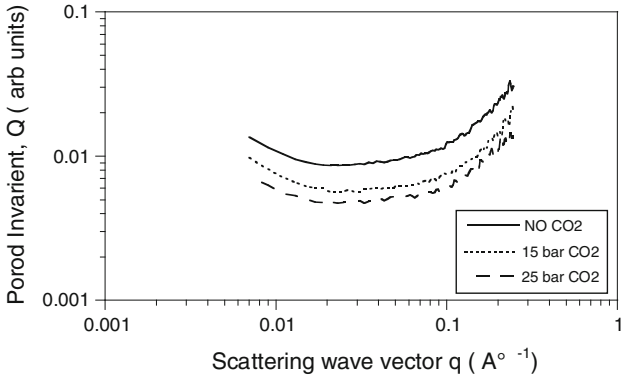

Fig. 6 $q^2I(q)$ verses q for SANS on Wyodak coal at various CO_2 pressures

Figure 5 shows Guinier plots for Wyodak coal at different CO_2 pressures. The absolute intensities at $q = 0$ are determined by the extrapolation of Guinier plots to $q = 0$ using Eq. 7. Analysis of Guinier plots by fitting to Eq. 7 is shown in embedded graph in Fig. 5.

The result of fitting gives the values of radius of gyration, R_g, calculated from Eq. 8 for the coal sample at different pressures. The geometrical radius, R_s, can be calculated from Eq. 6. The values of the R_g and R_s for Wyodak coal sample at various CO_2 pressures obtained by fitting of Guinier plots to Eq. 7 are given in Table 2.

R_g is a measure of the size of pores and represents only a rough, averaged dimension of the pores in the coal [24]. The results presented in Table 2 shows that the values of R_g grow with CO_2 pressure. A possible explanation for this might be the swelling of the coal associated with high-pressure CO_2.

Figure 6 shows a plot of $q^2I(q)$ versus q for Wyodak coal at different CO_2 pressures. Because the Porod's law behavior is not obeyed at the high q range, it was not possible to accurately estimate Porod invariant (Q).

The Porod invariant, Q, for the coal at various pressures is evaluated by the integration $\int I(q)q^2\,dq$ in the entire q range between 0 and 0.287 $\mathring{A}^{-1}$ as integrated area under the curves presented in Fig. 6. The values of calculated Porod invariants are given in Table 2. These values are not the exact values; however, they give a rough indication of the total porosity and the comparative scattering interfacial areas of the sample in various CO_2 pressures. The results given in Table 2 show that Q values increase with pressure, indicating increase in the total porosity of the Wyodak coal with CO_2 pressure that might be due to the swelling or extraction of coal by high-pressure CO_2.

Time dependence of the SANS patterns for Wyodak coal in high-pressure CO_2

Figure 7 compares SANS for fresh Wyodak coal and the coal at 25 bar CO_2 for various times. As can be observed, the effect of 25 bar CO_2 is to reduce the scattering intensity considerably in a very short time (10 min). This shows that CO_2 can diffuse into the pore structure and access to the entire pores quickly. The drastic reduction in the scattering intensities for coal at 25 bar CO_2 compared with the intensities for fresh coal is attributed to the reduction in the scattering contrast between pores and coal matrix due to pore filling with high-pressure CO_2. It can also be seen that the amount by which scattering intensity is reduced increases with q that might be due to the variations of the density of CO_2 with pore size.

The scattering curves for Wyodak coal under 25 bar CO_2 at different times show an increase in scattering intensities with time for $q > 0.03$ $\mathring{A}^{-1}$ after 10 min. A magnified representation of variations of scattering intensities with time is shown in embedded graph in Fig. 7. There are two possible explanations for increase in the scattering intensities with time. One can be the change in the coal structure and swelling of coal caused by high-pressure CO_2 dissolved in the coal matrix [12]. CO_2 is a fluid that can dissolve in the organic matrix and modify the physical and possible chemical structure of the coal matrix.

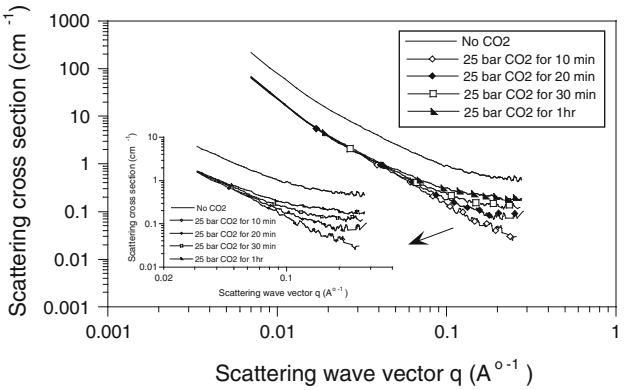

Fig. 7 Small angle neutron scattering patterns for Wyodak coal in 25 bar CO_2 for various times

This physical modification is associated with the relaxation and rearrangement of the macromolecular structure of coal and changes the pore structure of the coal with passing time [13]. An alternative explanation is that as CO_2 is adsorbed in micropores, it interacts with two pore walls and will be subjected to a large interaction energy or effectively a large pressure and behaves as a supercritical fluid [34]. Since the supercritical fluids have unique solubilizing and extracting properties, the increase in the scattering intensities in high q region might be attributed to the increase in micropore volume due to the extraction of organic matter from coal by supercritical CO_2. The SANS characteristics obtained by Guinier and Porod analysis of SANS patterns for Wyodak coal under 25 bar CO_2 at different times are given in Table 3. Increase in the values of the R_g and R_s with time given in Table 3 might be related to the further diffusion of CO_2 into the coal matrix with time, resulting in the increase in the coal porosity due to the swelling of the coal or the extraction of organic matter from the coal by high-pressure CO_2. Porod invariant is an indication of the void fraction and porosity of a porous material and, therefore, increase in Porod invariant with time indicates the development of porosity in the coal under high-pressure CO_2.

DSC results

The results of the calorimetric measurements of the adsorption process for nitrogen and carbon dioxide on Wyodak coal are shown in Figs. 8 and 9. The DSC results for the adsorption of N_2 on coal sample in Fig. 8 show that coal/N_2 interactions are very weak, and the adsorption of N_2 on coal occurs physically and reversibly.

Exothermic peaks for the adsorption of CO_2 on coal in Fig. 9 are associated with the uptake of CO_2. This is an activated process, and presumably at the temperature of the exotherms, there is enough thermal energy to overcome the activation energy for diffusion. A comparison between exotherms on Figs. 8 and 9 shows that interactions between coal and CO_2 are much stronger than those between coal and N_2.

The integrated values for the exotherms associated with the adsorption of CO_2 on Wyodak coal are given in Table 4. These values are indicative of the amount of CO_2 sorbed during the experiment. The reduction in the value of the exotherm between the first and second runs suggests that some CO_2 is irreversibly bound to the structure even after heating to 200 °C.

Structural change in Wyodak coal caused by high-pressure CO_2 is examined by studying the DSC thermograms of coal heated to 200 °C in nitrogen before and after exposure to high-pressure CO_2. Figure 10 shows DSC scans for dried Wyodak coal (before exposure) in N_2 atmosphere from 30 to 200 °C.

The first scan shows an irreversible process attributable to the enthalpy relaxation and structural rearrangement of the coal when heated above its glass transition temperature (T_g). The glass transition process is a reversible process presumably caused by the breakage of hydrogen bonds upon heating, and the reforming of them upon cooling [36]. Subsequent two scans after the first scan show a reversible

Table 3 SANS characteristics of the Wyodak coal under 25 bar CO_2 at various times

Time (min)	D_m	R_g (Å)	R_s (Å)	Q (arb. units)
0	2.62	197.70	255.23	0.0002064
10	2.86	210.68	271.98	0.0004175
20	2.79	218.02	281.46	0.0004723
30	2.72	222.38	287.09	0.0005519
60	2.65	231.80	299.25	0.0006472

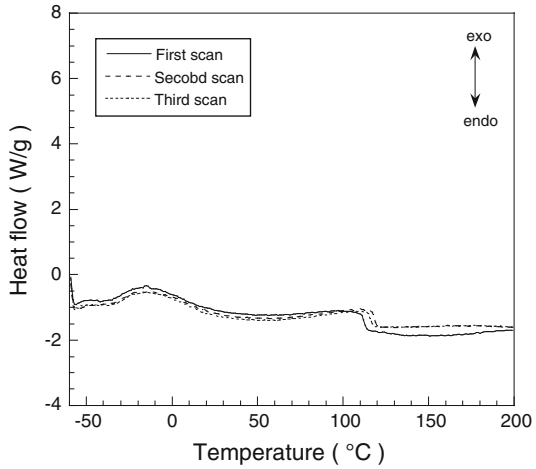

Fig. 8 DSC for Wyodak coal from −60 to 200 °C in N_2 atmosphere

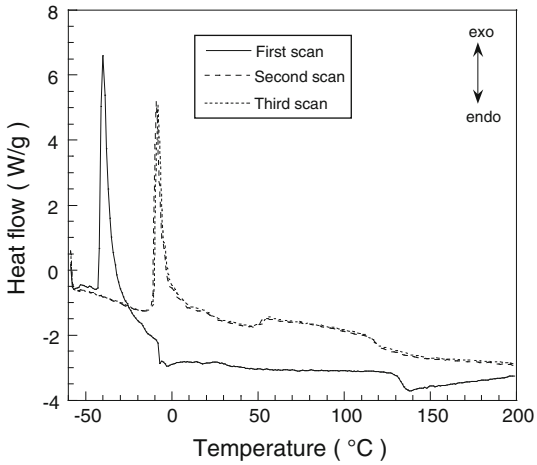

Fig. 9 DSC for Wyodak coal from −60 to 200 °C in CO_2 atmosphere

Table 4 Differential enthalpies of the adsorption of CO_2 on Wyodak coal

	First scan	Second scan	Third scan	Irreversible sorption capacity
ΔH (J/g)	27.40	20.60	18.72	6.8

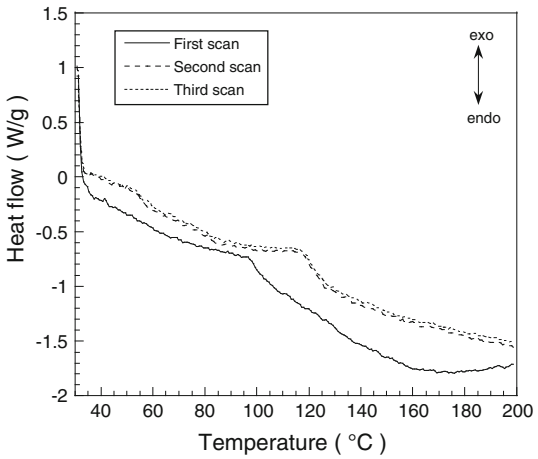

Fig. 10 DSC for Wyodak coal from 30 to 200 °C in N_2 atmosphere

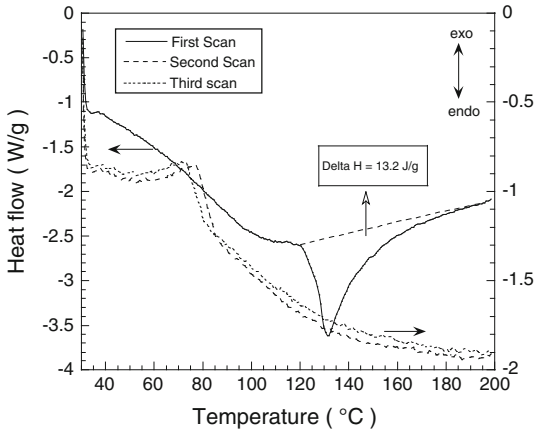

Fig. 11 DSC for Wyodak coal (held in 30 bar CO_2 for 24 h) from 30 to 200 °C in N_2 atmosphere

second-order process having the characteristics of glass transition in coal [9]. Before the transition, coal is a glassy solid with severely restricted macromolecular motions, and the diffusion of gases and liquids in its structure is slow. When heated to a certain temperature which is called glass transition temperature, a significant increase in coal's macromolecular motions happens. After the transition, coal becomes rubbery, and diffusion into its structure becomes much faster.

The DSC thermograms for dried Wyodak coal held under 30 bar CO_2 atmosphere for 24 h prior to the DSC measurements are depicted in Fig. 11. The first scan indicates two endothermic effects attributable to the continuous release of sorbed CO_2 since desorption process is endothermic, and to the fast release of absorbed CO_2 into the coal at the vicinity of the glass transition temperature, respectively. The coal sample in the DSC chamber will continuously release CO_2 during heating, and at the glass-to-rubber transition temperature, the desorption rate suddenly accelerates since the chain mobility of the coal suddenly becomes higher. This process is an irreversible process and has disappeared on the second and third scans. The second and third scans on Fig. 11 indicate a reversible process that has the characteristics of a glass transition temperature.

Figure 12 shows the DSC thermograms showing glass transition process for Wyodak coal held in CO_2 atmosphere at different pressures for 24 h.

The values of T_g of Wyodak coal at different pressures of CO_2 are given in Table 5. Glass transition temperatures

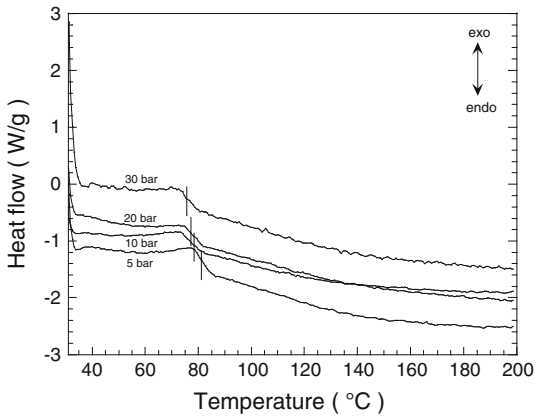

Fig. 12 DSC thermograms for Wyodak coal held in CO_2 atmosphere at different pressures for 24 h

are decreased from 121.1 °C for fresh coal to 75.7 °C for coal held under 30 bar CO_2 for 24 h. This shows that change in the structure of the coal caused by high-pressure CO_2 is significant.

There is a similarity between these results and the study of Mi and Zheng [37]. In their study, they have measured T_gs of polycarbonate in high-pressure CO_2 atmospheres and concluded that depression in T_g by high-pressure CO_2 is due to a strong plasticization of polycarbonate by CO_2. Chiou et al. [38] also studied plasticization of glassy polymers by CO_2 and reported that carbon dioxide at modest pressures causes significant reductions in the glass transition temperature of glassy polymers which have high CO_2 solubility. Coal has a polymeric character [9], and

Table 5 The glass transition characteristics of Wyodak coal at different pressures of CO_2

CO_2 pressure (bar)	Second scan T_g (°C)	Third scan T_g (°C)
0	121.1	121.6
1	117.2	114.2
5	86.6	81.7
10	83.2	78.2
20	82.4	77.8
30	81.1	75.7

depression in T_g in Wyodak coal with increase in CO_2 pressure might be in part due to the additional solubility of CO_2 in the macromolecular structure of coal matrix and plasticization of coal by CO_2. The solubility parameter (δ) is defined in terms of molar enthalpy of vaporization (ΔE) and the molar volume (v) as $\delta = (\Delta E/v)^{1/2}$. The solubility parameter of CO_2 will increase with increasing pressure due to a decrease in molar volume [10]. The further solubility of CO_2 into the coal with increase of pressure may thus be partly due to the solubility parameter of CO_2 approaching to a value closer to that of the coal.

Conclusions

In this study, the SANS and DCS are used to study the coal/CO_2 interactions and the effect of high-pressure CO_2 on coal macromolecular structure. Based on the experimental results, the following conclusions can be drawn:

(1) CO_2 rapidly adsorbs on and access entire pores in coal. Evidence for this is observed from the sudden decrease in the scattering intensities upon the introduction of CO_2 on coal observed on the SANS curves in the whole q range. This rapid adsorption is confirmed by the strong and steep exothermic peaks observed on DSC scans during coal/CO_2 interactions.

(2) SANS provides additional insights into the CO_2-induced macromolecular changes in coal's structure. Increase in the scattering intensities at high q range with exposure time in high-pressure CO_2 is an indication of structural change in the coal that might be due to the diffusion and solubility of CO_2 within the coal matrix or creation of additional microporosity in the coal structure. This can be explained by the swelling of coal caused by dissolved CO_2 at high pressures or extraction of organic matter from coal by adsorbed CO_2. Increase in the radius of gyration with CO_2 pressure and exposure time indicates that coal dimensions increase on exposure to high-pressure CO_2 suggesting that extent of swelling increases with increase in the CO_2 pressure and the exposure time. The DSC results also show that after the adsorption, CO_2 begins to diffuse into and change the macromolecular structure of the coal. The study of the coal macromolecular structure under high-pressure CO_2 by DSC revealed that high-pressure CO_2 causes significant plasticization in coal, enabling physical rearrangement of the coal's macromolecular structure and lowering its T_g significantly.

(3) The SANS patterns show that as CO_2 is adsorbed into pores in coal, the scattering intensities in the entire q range reduce significantly. The observed q dependence of the decrease in the scattering intensities after exposure to high-pressure CO_2 is thought to be due to the variation of the density of adsorbed CO_2 with pore size.

References

1. Survey of energy resources—executive summary (2007) World Energy Council, London
2. Mavor MJ, Robinson JR, Gale J (2002) SPE Paper 75683. Gas technology symposium 2002, Calgary, Canada
3. Ozdemir E, Schroeder K, Morsi BI (2002) Am Chem Soc Div Environ Chem Prepr 42:310
4. Shi JQ, Durucan S (2005) Oil Gas Sci Technol 60:547
5. White CM, Smith DH, Jones KL, Goodman AL, Jikich SA, LaCount RB, DuBose SB, Ozdemir E, Morsi BI, Schroeder KT (2005) Energy Fuels 19:659
6. Reeves S (2002) World Oil 223(12):56
7. Prusty BK (2008) J Nat Gas Chem 17:29
8. Gunter WD, Gentzis T, Rottenfusser BA, Richardson RJH (1997) Energy Convers Manage 38S:217
9. Karacan CO (2003) Energy Fuel 17(6):1595
10. Reucroft PJ, Patel H (1986) Fuel 65:816
11. Reucroft PJ, Patel KB (1983) Fuel 62:279
12. Reucroft PJ, Sethuraman AR (1987) Energy Fuels 1:72
13. Larsen JW (2004) Int J Coal Geol 57:63
14. Green TL, Kovac J, Brenner D, Larsen JW (1982) In: Meyers RA (ed) Coal Structure. Academic Press, New York, p 199
15. Larsen JW, Mohammadi M (1990) Energy Fuels 4:100
16. Mirzaeian M, Hall PJ (2006) Energy Fuels 20:2022
17. Robertson EP (2009) Int J Coal Geol 77:234
18. Ellis MS, Flores RM, Ochs AM, Stricker GD, Gunther GL, Rossi GS, Bader LR, Schuenemeyer JH, Power HC (1999) U.S. Geological Survey Professional Paper 1625-A, p 84
19. Winans RE, Thiyagarajan P (1988) Energy Fuels 2:356
20. King SM (1999) In: Pethrick RA, Dawkins JV (eds) Modern techniques for polymer characterization. John Wiley & Sons, p 171
21. Hall PJ, Brown SD, Calo JM (2000) Fuel 79:1327
22. Guinier A, Fournet G (1995) Small angle scattering of X-ray. John Wiley & Sons, New York
23. Kostorz G (1979) Treatise on materials science and technology, vol 15. Academic Press, New York
24. Gethner JS (1986) J Appl Phys 59:1068
25. Higgins JS, Benoit HC (1994) Polymers and neutron scattering. Clarendon Press, Oxford

26. Gregg SJ, Sing KSW (1967) Adsorption, surface area and porosity. Academic Press, New York
27. Rouquerol F, Rouquerol J, Sing K (1999) Adsorption by powders and porous solids, principles, methodology and applications. Academic Press, New York
28. Tanaka R, Hunt JE, Winans RE, Thiyagarajan P, Sato S, Takanohashi T (2003) Energy Fuels 17(1):127
29. Ramsay JDF (1998) Adv Colloid Interface Sci 76–77:13
30. Hall PJ, Brown S, Fernandez J, Calo JM (2000) Carbon 38:1257
31. Larsen JW, Hall PJ, Wernett PC (1995) Energy Fuels 9:324
32. Foster MD, Jensen KF (1990) J Colloid Interface Sci 135:132
33. Hall PJ, Ruiz Machado W, Gascon Galan D, Barrientos Barria EL, Sherrington J (1996) Chem Soc, Faraday Trans 92:2607
34. Meyers RA (1982) Coal structure. Academic Press, INC., New York
35. Mondragon F, Quintero G, Jaramillo A, Fernandez J, Calo JM, Ruiz W, Hall PJ (1997) J Mater Sci 32(6):1455. doi:10.1023/A:1018549800150
36. Mackinnon AJ, Antxustegi MM, Hall PJ (1994) Fuel 73(1):213
37. Mi Y, Zheng S (1998) Polymer 39:3709
38. Chiou JS, Barlow JW, Paul DR (1985) J Appl Polym Sci 30:2633